15

FERMILAB
JAN 26 1998
LIBRARY

KEK Report 97-11
November 1997
A

Beam-based Measurement of the Strength Deviation of Quadrupole Fields in the TRISTAN Main Ring

KEK-REPORT-97-11

Fermilab Library
0 1160 0059737 1

S. MATSUMOTO, H. KOISO and S. KAMADA
KEK, Tsukuba

NAME	I.D.No.	M.S.

High Energy Accelerator Research Organization

** From April 1, 1997, **High Energy Accelerator Research Organization (KEK)** was newly established. The new organization is restructured of three reseach institutes, National Laboratory for High Energy Physics (KEK), Institues of Nuclear Study (INS), Univ. of Tokyo and Meson Science Laboratory, Faculty of Science, Univ. of Tokyo.*

© High Energy Accelerator Research Organization (KEK), 1997

KEK Reports are available from:

Information Resources Division
High Energy Accelerator Research Organization (KEK)
1-1 Oho, Tsukuba-shi
Ibaraki-ken, 305
JAPAN

Phone: 0298-64-5137
Fax: 0298-64-4604
Cable: KEK OHO
E-mail: Library@kekvax.kek.jp (Internet Address)
Internet: http://www.kek.jp

Beam-based measurement of the strength deviation of quadrupole fields in the TRISTAN Main Ring

Shuji Matsumoto, Haruyo Koiso, Susumu Kamada

KEK, High Energy Accelerator Research Organization

1-1 Oho, Tsukuba, Ibaraki 305, Japan

Abstract

The deviation of focusing strength of quadrupole magnets from their design value were measured by a beam-based method, the "π-bump method" in the TRISTAN main ring. Small deviation as much as 0.1% was successfully observed.

1 Introduction

In the machines such as high luminosity colliders or low emittance light sources, even smaller errors of machine components may significantly degrade their ultimate performance. In order to achieve high performance, beam-based diagnostics of machine errors is really important, as well as careful quality control of hardware components. The π-bump method is one of the beam-based diagnostics utilizing a π-bump orbit to detect a tiny error of the magnets.

A π-bump is a local bump excited by a pair of correction dipole magnets (correctors) between which the designed betatron phase advance is exactly π radian. If the phase advance is actually π, the bump orbit can be completely confined within the short section between the correctors. Otherwise it indicates the disturbance of the optics within the section. A possible source of the disturbance is a quadrupole magnet whose strength is deviated from

its design values. From the size of the "leakage orbit", we can estimate the deviation.

As we will see below, the π-bump method is very sensitive, since it fully utilizes special relations of betatron phase between the magnets. We have applied this method in the TRISTAN main ring (MR) to measure the strength deviation of quadrupole magnets [4] as well as the misalignment of sextupole magnets [5]. In this paper, we will report the former results in detail. This paper is organized as follows. In the next section, we will review briefly the π-bump method. Section 3 is a note on our measurement and analysis. In section 4, results and discussions are given. The last section is devoted to the conclusion. The discussion of the orbit length effect by the π-bump is given in Appendix.

2 A Brief Review of the π-bump Method

We only use the linear orbit theory [1] here. The discussion in this section is essentially the same as that given in Refs. [2, 4].

2.1 π-bump

Suppose a storage ring with the circumference C. The azimuthal coordinate s $(0 \leq s < C)$ is along the design orbit of the ring. A distorted orbit, $x(s)$, produced by a single thin correction dipole magnet (corrector) located at $\bar{s}$ is [1]

$$x(s) = \frac{k\ \beta^{1/2}(s)\ \beta^{1/2}(\bar{s})}{2\sin\pi\nu}\ \cos(|\psi_{\bar{s}}(s)| - \pi\nu) \quad (\text{for}\ \ 0 \leq s < C), \tag{1}$$

where k is the kick angle of the corrector magnet, $\beta^{1/2}(s) = \sqrt{\beta(s)}$ and β is the betatron function, $\psi_{\bar{s}}(s)$ is the betatron phase advance from $\bar{s}$ to s and ν is the betatron tune. This orbit has a kink at $\bar{s}$, where the derivative $x'\,(= dx/ds)$ jumps by k. A π-bump is made by two correctors. Let them be ST1 and ST2, located at s_1 and s_2 $(s_2 > s_1)$ and their kick angles are k_1 and k_2 respectively. We call the region between the correctors, $s_1 < s < s_2$, the bump region, otherwise outside region. From Eq. (1), the distorted orbit by

ST1 and ST2 in the outside region is

$$x(s) = A\frac{\beta^{1/2}(s)}{2\sin\pi\nu}\cos(\psi_{s_1}(s) - \pi\nu - \theta) \quad (\text{for } s_2 < s < C), \tag{2}$$

where

$$A = \sqrt{{Z_1}^2 + {Z_2}^2 + 2Z_1Z_2\cos\chi}\,, \tag{3}$$

$$\tan\theta = \frac{Z_2\sin\chi}{Z_1 + Z_2\cos\chi}\,. \tag{4}$$

Here $Z_i = \beta^{1/2}(s_i)\,k_i$ $(i = 1, 2)$ and χ is the phase advance within the bump region. The amplitude A is zero *if* and *only if*

$$\chi = n\pi \quad (n = 1, 2, 3, \ldots) \tag{5}$$

and

$$Z_1 = (-1)^{n+1}Z_2 \equiv Z, \tag{6}$$

are fulfilled at the same time. When $n = 1$, the orbit along the whole ring is confined within the bump region:

$$x_0(s) = \begin{cases} Z\,\beta^{1/2}(s)\,\sin\psi_{s_1}(s) & \text{in the bump region,} \\ 0 & \text{outside.} \end{cases} \tag{7}$$

As the phase advance in the bump region is π, we call this localized bump a π-bump. Notice that the height of a π-bump is proportional to Z. The corrector kick angles are a knob to control it.

2.2 Beam-based diagnostics utilizing a π-bump

Now let us discuss the π-bump method, the method to measure an optics error by a π-bump orbit. Suppose we make a π-bump by ST1 and ST2 located at $s = s_1$ and $s = s_2$. If there is a localized small focusing error δg in the bump region, it violates the condition $\chi = \pi$. In this case, even though the correctors are balanced, we have a *leakage orbit* outside the bump region. The leakage orbit can be easily obtained to the first order of δg as follows. Let t $(s_1 < t < s_2)$ be the location of δg. Suppose we excite ST1 and ST2 in such a way that they satisfy Eq. (6). The bump orbit at t differs from

Eq. (7) since δg changes the optics of the ring. However, the difference is the order of δg. Thus $h = x_0(t) + O(\delta g)$, where h is the bump height at t. The leakage orbit of our concern is the distorted orbit by the additional kick or *miskick* at t which amounts to $h\delta g$. From Eqs. (1) and (7), the leakage orbit is

$$x(\delta g, t|s) = \delta g \frac{Z\beta^{1/2}(s)}{2\sin\pi\nu} \{w_c(t)\cos(\psi-\pi\nu)+w_s(t)\sin(\psi-\pi\nu)\}+O(\delta g^2), \quad (8)$$

where ψ stands for $\psi_{s_1}(s)$. We decompose the leakage orbit into two linearly independent components: the cosine and sine components. The amplitude of each component is characterized by the weight function, w_c or w_s, both of which are defined in the bump region.

$$w_c(s) = \beta(s)\,\sin\psi\cos\psi, \quad w_s(s) = \beta(s)\,\sin^2\psi, (s_1 < s < s_2). \quad (9)$$

The weight function determines the contribution of δg to each component of the leakage orbit.

We have assumed the correctors are completely balanced. If this breaks, we have a leakage orbit too. Let $\beta^{1/2}(s_1)\,k_1 - \beta^{1/2}(s_2)\,k_2 = \delta Z$, while $\chi = \pi$. From Eq. (2), the leakage orbit due to the unbalance is

$$x(\delta Z|s) = \delta Z \frac{\beta^{1/2}(s)}{2\sin\pi\nu} \cos(\psi_{s_1}(s) - \pi\nu). \quad (10)$$

Note that the unbalance gives only the cosine component.

2.3 π-bumps in TRISTAN MR

In Fig. 1, the vertical bump orbit and the weight functions w_c and w_s in a normal cell of the TRISTAN MR are shown. There is a quadrupole magnet in the middle of the bump region where w_s is almost its maximum. We call this magnet the target. There are three quadrupole magnets except the target in the bump region, however, w_s has relatively small value at these magnets. In other ward, the leakage orbit is sensitive to the strength error of the target. Note that w_c is almost zero at the target. The error of the target can be known from the sine component and this component gets away from the unbalance of correctors.

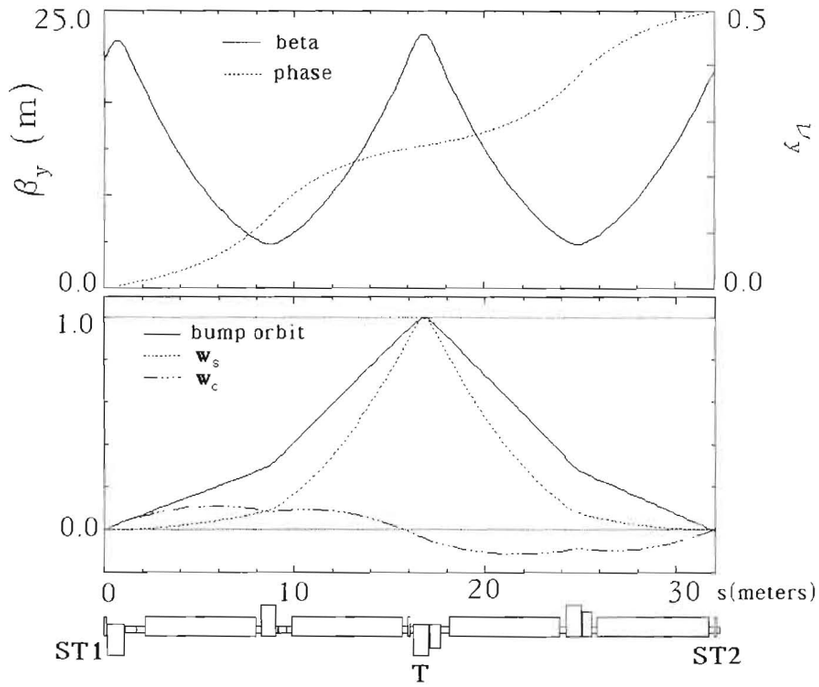

Figure 1: The vertical π-bump orbit in the arc of the TRISTAN MR. The lattice configuration (FODO) is given at the bottom. The phase advance of the unit cell is designed to be $\pi/2$. (Upper figure) The solid line is $\beta^{1/2}$ and the dashed line is the phase advance $\psi_{s_1}(s)/2\pi$. (Lower figure) The solid line is the geometrical shape of the bump orbit and the dashed and dash-dot lines are the weight functions. They are normalized by their maximum values. (The maximum of w_c is smaller than that of w_s. Thus w_c is normalized by the latter.) The defocusing quadrupole magnet T is the target. The design phase advance from ST1 to ST2 is exactly π.

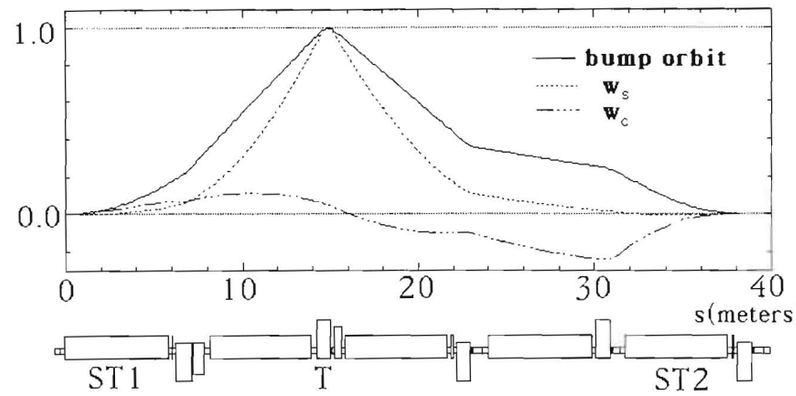

Figure 2: The geometrical shape of a horizontal bump orbit and its weight functions in a normal cell of TRISTAN MR. Both of them are normalized by their maximum values. Since ST1 and ST2 are 5.86 meters long, the bump orbit and the weight function are "slanted". The target T is a focusing quadrupole magnet, which locates at w_s being almost its maximum.

The vertical corrector is very thin (0.1 m long), while the horizontal corrector in the arc is long, since we use the bending magnet (5.86 m long) as a corrector by the correction coil. We show how a horizontal π-bump in the normal cell looks like in Fig. 2. We also show the weight functions. We find a quadrupole magnet which is appropriate as the target of this bump too. This π-bump can be used to estimate its strength deviation.

Note that in the case the long uniform correctors being used, the π-bump is closed when the condition

$$\int_{\mathrm{ST1}} ds_1 \int_{\mathrm{ST2}} ds_2 \;\; T_{12}(s_1|s_2) = 0, \tag{11}$$

is fulfilled instead of Eqs. (5). Here $T_{12}(s_1|s_2)$ is the (1,2)-component of the (horizontal) transfer matrix from s_1 to s_2, where s_1 is a point on ST1 while s_2 is on ST2, and the integration is done over whole ST1 and ST2.

3 Measurement

3.1 Optics

A specially designed optics was set for our measurement. The lattice of the TRISTAN MR consists of colliding insertions, rf sections, dispersion suppressers, arcs and wiggler sections. The arcs consists of FODO cells whose

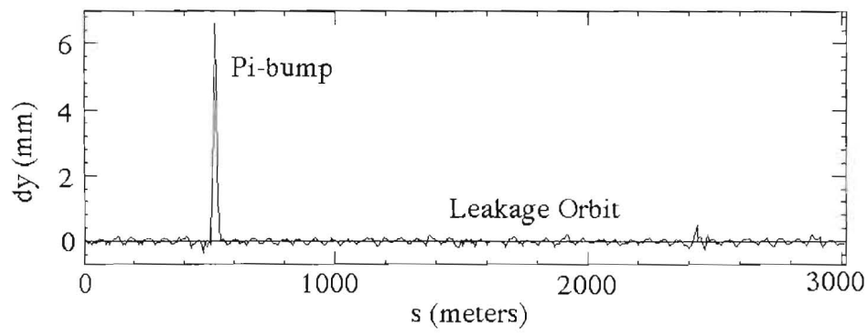

Figure 3: An example of the observed leakage orbit, obtained by subtracting *Orbit A* from *Orbit B*. In this example, we set a positive(upward) vertical π-bump. The bump height at the target is about 6 mm. The leakage orbit is clearly seen.

phase advance was set to be 90/90 degrees during this study. The $\pi/2$ normal cell is suitable for the π-bump measurement. As shown in Fig. 1 and Fig. 2, π-bumps in the arcs can be made by giving the same excitation to two correctors at the identical position in every second cell. We turned off all the sextupole magnets during the measurement, in order to get rid of the side effects on the orbit by them.

3.2 Measurement of the leakage orbits

The orbit around the ring is measured by 392 position monitors attached to quadrupole magnets. The leakage orbit can be known by comparing the orbits of the bump being on and off. We measured three orbits sequentially for a single bump: the first orbit measurement was done *before* the bump being on (*Orbit A*), the second orbit was measured when the bump was on (*Orbit B*) and the last one was done *after* the bump being off (*Orbit C*). By subtracting *Orbit A* from *Orbit B*, we have a leakage orbits to be analyzed. Similarly, from *Orbit C* and *Orbit B*, we have another leakage orbit. If we observe significant difference between these two leakage orbit, we rejected the data. An example of the observed leakage orbit is shown in Fig. 3.

3.3 Analysis

We summarize the prescriptions of our data analysis for the leakage orbit.

Contributions from other quadrupole magnets We neglect the contribution from other quadrupole magnets except the target in our analysis. This enables us to estimate δg of the target individually per bump.

A virtual corrector at the target The observed leakage orbits were analyzed by Eq. (8) to estimate δg. We utilize the orbit correction code in SAD [6] for the fitting process. We insert a virtual thin corrector in the lattice deck for SAD at an edge of the target and "correct" the observed leakage orbit by this corrector. The correction kick angle by this virtual corrector can read (the opposite sign of) the miskick angle due to the focusing error of the target.

4 Results and Discussions

4.1 Statistical error of the measurement

Since we switched off all the sextupole magnets during the measurement, the stored beam current was very low (typically the total current was 0.1 mA by 8-bunch operation) and this causes the S/N ratio of the orbit measurement system to be lowered. We checked the noise level in our system was done by measuring the same orbit twice (We measure an orbit and measure it again immediately after the first measurement is done). We have taken 55 samples of "noise orbits", the difference between the two successive measurements, and we "correct" these noise orbits by the virtual corrector.

The result is shown in Fig.4. We find that the correction kick angles (by the virtual corrector) distribute over the range whose standard deviation is about 0.2 μrad. This value is the typical size of the statistical error included in our analysis coming from the noise in the measurement system. Note that this error is small but not negligible compared with the typical size of the miskick by the targets. For example, suppose the height is 10 mm and deviation is 0.1%. The beam gets a miskick of 1.8 μrad. In this example, the statistical error, 0.2 μrad, amounts to about 10% of the target miskick.

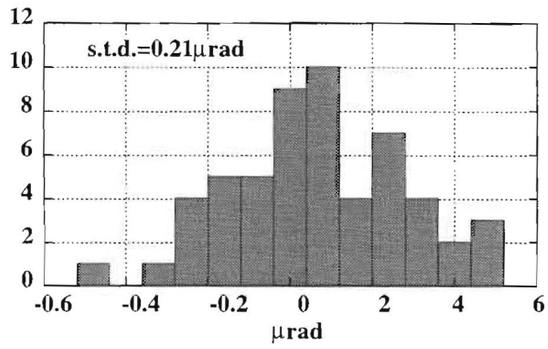

Figure 4: The statistical error in the estimation of the miskick due to the noise in the orbit measurement system. The distribution of the miskicks obtained by a virtual corrector for the 55 samples. The standard deviation of the distribution of the kick angle is about 0.2 μrad.

4.2 Precise measurement

If we repeat the orbit measurement several times for a single target by changing the bump height, the measurement will be more reliable. However we aimed to check as many quadrupole magnets as possible within a limited machine time. Therefore, we choose only several magnets in the arcs for the precise measurement.

In Fig. 5, the result of precise measurement for a QF magnet in the arc is shown. The observed horizontal miskick angle by the target QF does not show a linear dependence on the horizontal bump height. A possible source of the nonlinear kick is the focusing sextupole magnet, SF, next to the target. All of the sextupole magnets are off during the measurement but there remains remnant field in it. A parabola fit to the present data estimates the integrated sextupole field to be $K_{2,\ SF}^{(\mathrm{rem})} = (3.2 \pm 0.3) \times 10^{-2}$, which agrees well with the direct field measurement, which shows $K_{2,\ SF}^{(\mathrm{rem})} = 2.9 \times 10^{-2}$ [3]. The linear component of the kick is 0.40 ± 0.01 μrad per 1 mm bump height which reads +0.22% strength deviation of the target, if we suppose this linear kick is coming from the target only.

However, the remnant field in SF can also give the linear kick like

$$\delta x' = K_{2,\ SF}^{(\mathrm{rem})}\ x_{\mathrm{off}}\ h_x, \tag{12}$$

where x_{off} and h_x are the horizontal misalignment of the sextupole magnet and the bump height respectively. The linear kick in Eq. (12) and that by the target are nor separable unless x_{off} is known. The remnant field can be

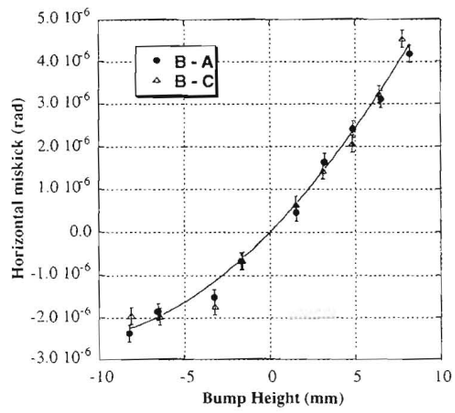

Figure 5: The plots of the miskick by a QF in the arc against the horizontal bump height. The data of *Orbit B-Orbit A* and *Orbit B-Orbit C* are shown. Some bad data were rejected. The error bars indicates the statistical error due to the noise in our orbit measurement system, discussed in the previous section. Due to the remnant field of SF next to the target, the miskick is not proportional to the bump height.

a source of uncertainty in the estimation of the strength deviation of QF. For example, suppose $x_{\text{off}} = 1$ mm. This is actually an extreme case. If we make a $h_x = 10$ mm bump, the size of the kick amounts to 0.4 μrad, which introduces a few tens % uncertainty in the estimation of the target miskick given above.

The miskick due to QD strength deviation is, on the other hand, proportional to the vertical bump height as it should be. See the left picture of Fig. 6. The linear fit gives the vertical miskick is -0.20 μrad per 1 mm bump height (the statistical error is less than 0.01 μrad/mm) and this reads the focusing strength of the target QD is deviated as much as -0.11% from its design value. However, we should check the remnant field in a defocusing sextupole magnet SD, which is next to the target, since it also gives the linear kick as the bump height being changed. The remnant field can be known by the plots of the *horizontal* leakage orbit against the vertical bump height. See the right picture of Fig. 6. A parabola fit shows the integrated field strength of SD is $K_{2,\,SD}^{(\text{rem})} = -(3.4 \pm 0.2) \times 10^{-2}$. (The direct measurement shows $K_{2,\,SD}^{(\text{rem})} = -3.9 \times 10^{-2}$.) The remnant field in SD magnets also gives

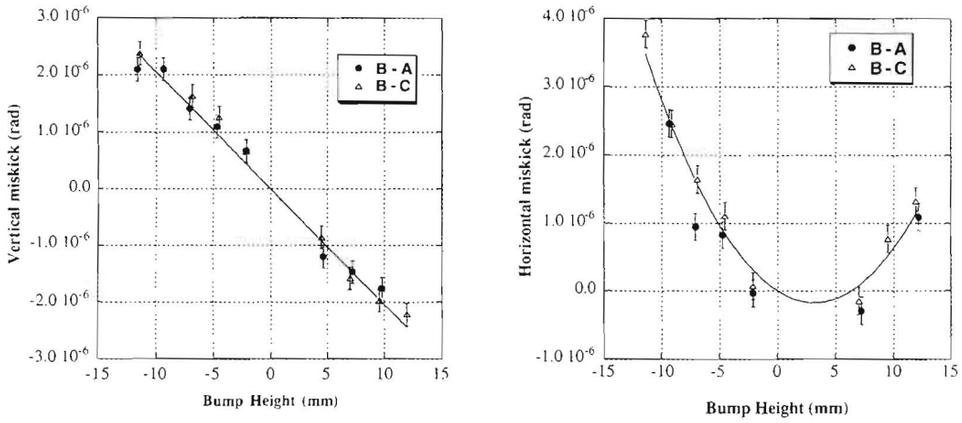

Figure 6: The miskick of a QD in the arc against the bump height. (Left) the vertical miskick. (Right) Horizontal kick. A possible source of the horizontal miskick is the sextupole magnet next to the target. The shift of the minimum of parabola from the origin indicates its misalignment.

uncertainty to the result of QD magnets.

4.3 Distribution of the strength error

We measured 220 out of 400 quadrupole magnets in the ring by only one bump. They are 76 QF (horizontally focusing) magnets and 80 QD (horizontally defocusing) magnets in the arcs and 64 in the straight sections. Note that the QF magnets are fed by a single power supply and also are the QD magnets. Quadrupole magnets in the dispersion suppressers and wiggler sections remain unmeasured since the optics is not adjustable to make π-bumps there. The typical bump height was 10mm.

Figure 7 shows the distributions of the relative strength deviation of the quadrupole magnets. In these measurements, we applied only one bump for one quadrupole magnet. As for QF and QD magnets, the data is corrected by the subtracting the kick component due to sextupole remnant field. As for Q_{IR} magnets, there is no sextupole magnet next to them.

The standard deviations of the strength (K value) error of QF and QD magnets are 5.7×10^{-4} and 5.9×10^{-4}, respectively, which are consistent with

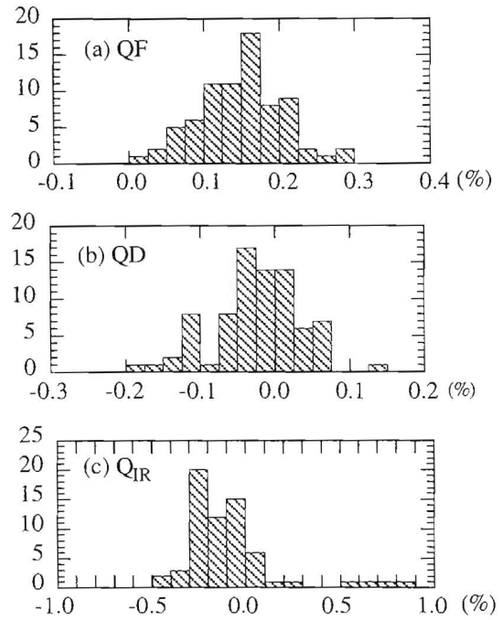

Figure 7: Relative strength deviation of the quadrupole magnets in MR. a) QF magnets b) QD magnets and c) quadrupole magnets in the straight sections.

that obtained from the field measurement done before the installation [3]. Large error was observed in final quadrupole magnets in the colliding insertions. We measured these magnets as much lower excitation than that during usual operations. At the usual excitation, the deviations of these magnets become similar to the others in the straight sections.

4.4 Comments on the correction of strength error

A π-bump can be used in not only detecting the small focusing error but correcting it. We did not try to correct the focusing error actually this time. We just make a few comments on the procedure to do it.

Suppose only the target has the focusing error in the bump region. Then we can correct its focusing error by changing the strength of the target with observing the leakage orbit. If the leakage orbit disappears, the correction is done. Of course, this is not the case: the target is not the only the source of focusing error within the bump region in general. At least other quadrupole magnets in the bump region can be the sources too. Mathematically speaking, we can complete the correction if we have the individual leakage orbits

whose number are equal to or larger than the number of the sources of focusing error. As shown in Figs. 1 and 2, the target has dominant contribution to the leakage orbit. The target is the most suitable magnet for the correction of the local optics within the bump region.

5 Conclusion

We are confident that the π-bump method works fine to detect a tiny optics error. We demonstrated its sensitivity was down to $\sim$1 μrad. The deviation of the quadrupole magnets is rather small and the measurement of the deviation is suffered by the contribution from the sextupole remnant fields. The precise measurement, i.e., to measure several orbit by changing the bump height, is essential to filter out the contribution from the remnant fields. The correction scheme for the quadrupole magnets is promising.

Acknowledgments The authors would thank TRISTAN Operation Group for supporting the study. They would appreciate K. Oide, N. Yamamoto, M. Kikuchi, H. Fukuma and Y. Funakoshi for useful discussions.

References

[1] See, for example, M. Sands, "The Physics of Electron Storage Rings", SLAC-121 (1970).

[2] S. Kamada, Tristan Memo 398 (unpublished, in Japanese)

[3] N. Kumagai, K. Egawa, K. Takayama and M. Kihara, IEEE Trans. Magnet **24** 1319 (1988).

[4] H. Koiso, et al. in Proc. of Euro. Part. Accel. Conf. (1996).

[5] N. Yamamoto, et al.in Proc. of Euro. Part. Accel. Conf. (1996).

[6] SAD is an accelerator modeling program developed at KEK. Check http://130.87.74.156/SAD/sad.html for more information.

Appendix *Change of the path length by π-bump*

When we apply an outward (inward) horizontal π-bump in the arcs, the length of the orbit outside the bump region should be shortened (lengthened) so that the total orbit length is kept constant. We still have a leakage orbit even though the optics in the bump region is perfect[1]. In general, the change of the orbit length by a horizontal bump is given as $\delta L = \int (x/\rho)\, ds$, where x is the orbit deviation by the bump and ρ is the curvature radius of the design orbit. The integration is done over the whole ring. From Eq. (7),

$$\delta L = Z \int_{\text{bump}} \frac{\beta^{1/2}(s) \sin \psi(s)}{\rho(s)}\, ds, \tag{13}$$

where the integration is done over the bump region. Notice that δL is proportional to Z. Substituting designed β and ψ in Eq. (13), we found δL is $+0.65$ mm per 1 mrad outward corrector kick. The path length outside of the bump region is changed by the same amount. The leakage orbit due to this effect is proportional to the dispersion function, $x(s) = \epsilon\, \eta(s)$ and we have $\epsilon = -2.8 \times 10^{-4}$ per 1 mrad corrector kick outward[2]. In Fig. 8, the orbit observed by a horizontal π-bump in the arc is shown.

We consider $\bar{x}$, which is the average of the data of the orbit deviation observed at the monitors in the outside region. We expect $\bar{x}\,(= \epsilon\, \bar{\eta})$ is -81.0 μm per 1 mrad from the model while the experimental data shows it is -86.8 μm per 1 mrad. See Fig. 9. Experimental result agrees well to our expectation: it is about 7% larger than the model prediction.

[1] A vertical bump should have this effect too, but it is very small.

[2] The momentum compaction of the model is 7.76×10^{-4} and its design orbit length is 3018 m.

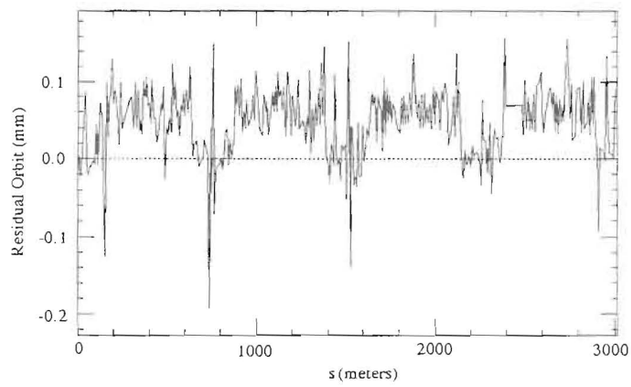

Figure 8: An example of observed leakage orbit by the horizontal bump. Although the data is noisy, we can see the orbit waves four times along the ring and it looks like the dispersion.

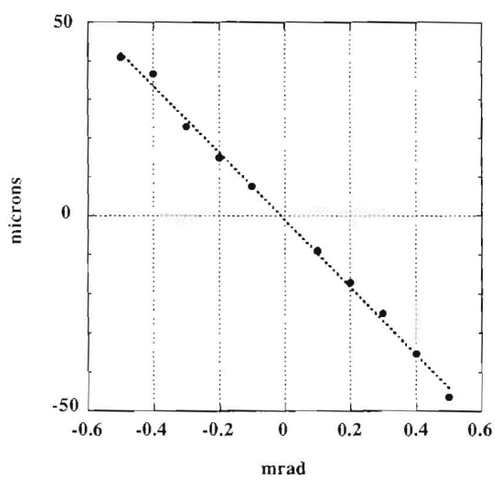

Figure 9: The mean orbit drift outside the bump region $\bar{x}$ against the kick angle of the corrector magnets. The linear fit is good. The data shows that the mean drift is -86.8 μm per 1 mrad corrector kick.